Translational and Rotational Contributions to the Quadrupole-Induced Dipole Absorption in Liquid CS_2

Hubert Stassen[†] **and William A. Steele***[,†,‡]

Departamento de Física-Química, Instituto de Química, Universidade Federal do Rio Grande do Sul, Av. Bento Gonçalves, 9500, 91540-000 Porto Alegre-RS, Brazil, and Department of Chemistry, Pennsylvania State University, University Park, Pennsylvania 16802

Received: January 7, 1997; In Final Form: May 8, 1997[⊗]

Molecular dynamics computer simulations of CS_2 at 298 K and vapor−liquid coexistence have been utilized to calculate time correlation functions for the velocities (time derivatives) of the quadrupole-induced dipole moments in the liquid. It is shown that the correlation functions for these dipole velocities can be used to reproduce the corresponding time correlation functions for the dipole moments. The velocity time correlation functions give an insight into the translation−rotation coupling in this liquid, especially in connection with the spectral time correlation functions corresponding to far-infrared absorption. The time derivative two-, three-, and four-body contributions to the spectral correlation functions are evaluated, and the relative importance of the translational and the various rotational contributions to these and the collective functions is discussed.

I. Introduction

The interaction-induced (II) contributions to absorption or light scattering spectra of liquids are often referred to as translational−rotational spectra. In the framework of classical mechanics, the corresponding time correlation functions (TCFs) depend on the time evolution of quantities that are functions of the individual positions and orientations of the N particles composing the fluid. Usually, the discussion of the spectral TCFs has been restricted to the time evolution of the configurational quantities that produce the induced dipole moments. Specifically, the spectral TCFs for II infrared absorption are those for the dipole moments induced by molecular electric fields interacting with polarizable molecules in the fluid. Although the relevant TCF can readily be obtained by computer simulation, the complexity of the problem is a barrier to the generation of physical insights into the molecular dynamic processes that play a significant role in the determination of these TCFs. Specifically, the magnitudes and decays of these functions depend upon both translational and rotational motion and furthermore, the many-body nature of II dipole moments means that two-, three-, and four-body TCFs are present in principle and, based on simulations carried out previously, in practice. Here, we investigate a rigorous reformulation of the problem that shows promise of separating the problem into its component translational and rotational parts via the time derivatives. It is known that the description of such TCFs by time derivatives might simplify their theoretical treatment,[1] but only recently have approaches to spectral TCFs via the normal mode picture of liquids raised the need for a discussion of the corresponding velocity terms.[2,3] In the present article, we present second time derivative TCFs of quadrupole-induced dipole (QID) moments obtained from molecular dynamics (MD) simulations of liquid CS_2 and demonstrate how terms containing linear and angular velocities of the molecules are involved in the collective spectra for that induction mechanism.

A general description of the reformulation used here has been given elsewhere.[4] We show how the spectral TCF is transformed in this approach. Thus, the TCF for the system's total dipole moment $\mathbf{M}$ is given by the canonical average, denoted by $\langle ... \rangle$, of the scalar product between $\mathbf{M}$ at some initial time $t = 0$ and $\mathbf{M}$ at time t:

$$C(t) = \langle \mathbf{M}(0) \cdot \mathbf{M}(t) \rangle \tag{1}$$

One writes

$$\mathbf{M}(t) = \mathbf{M}(0) + \int_0^t \dot{\mathbf{M}}(t')\, dt' \tag{2}$$

and the equivalent relation for the dipole velocities $\dot{\mathbf{M}}$ in terms of the second time derivative of $\mathbf{M}$. Substituting eq 2 and the corresponding equation of motion for the dipole velocities into the TCF of eq 1, one finds

$$C(t) = C(0) + t\langle \mathbf{M}(0) \cdot \dot{\mathbf{M}}(0) \rangle + \int_0^t dt' \int_0^{t'} \langle \mathbf{M}(0) \cdot \ddot{\mathbf{M}}(t'') \rangle\, dt'' \tag{3}$$

By use of the properties of TCFs for classical variables,[5] $\langle \mathbf{M}(0) \cdot \dot{\mathbf{M}}(0) \rangle = 0$ and $\langle \mathbf{M}(0) \cdot \ddot{\mathbf{M}}(t) \rangle = -\langle \dot{\mathbf{M}}(0) \cdot \dot{\mathbf{M}}(t) \rangle$ and by partial integration with respect to t', the TCF of eq 1 can be written in terms of its second time derivative $C^{(2)}(t)$:

$$C(t) = C(0) - \int_0^t (t - \tau) C^{(2)}(\tau)\, d\tau \tag{4}$$

with $C^{(2)}(t)$ being the TCF for the dipole velocities

$$C^{(2)}(t) = \langle \dot{\mathbf{M}}(0) \cdot \dot{\mathbf{M}}(t) \rangle \tag{5}$$

Equations 4 and 5 show how one can compute the TCF for $\mathbf{M}$ from a knowledge of the velocities $\dot{\mathbf{M}}$. In fact, one can write

$$\dot{\mathbf{M}} = \sum_I \dot{Q}_I \frac{\partial \mathbf{M}}{\partial Q_I} \tag{6}$$

where the Q_I denote the coordinates, translational and orientational, that appear in the expression for $\mathbf{M}$ and, of course, the $\dot{Q}_I$ are the corresponding velocities. Consequently,

$$C^{(2)}(t) = \sum_I \sum_J \left\langle \dot{Q}_I(0) \frac{\partial \mathbf{M}(0)}{\partial Q_I} \dot{Q}_J(t) \frac{\partial \mathbf{M}(t)}{\partial Q_J} \right\rangle \tag{7}$$

It can now be seen that $C^{(2)}(t)$ is a sum of TCFs that, depending

[†] Universidade Federal do Rio Grande do Sul.
[‡] Pennsylvania State University.
[⊗] Abstract published in *Advance ACS Abstracts,* October 1, 1997.

S1089-5647(97)00096-5 CCC: $14.00

upon I and J, involves separate TCFs involving translational and rotational velocities as well as rigorously defined translation−rotation cross terms. Note that the relative magnitudes and time decays of all these terms depend upon the property (here, equal to **M**, which itself depends upon the specific induction mechanism) and, as will be shown below, upon the n-body nature of this property. Thus, this approach shows that translation−rotation coupling or the relative importance and time decays of translation and rotation for a given liquid at a given temperature depend upon the property being studied—an obvious point, but one that has been occasionally overlooked in previous work.

In order to better understand the representation of spectral TCFs by functions of linear and angular velocity, the collective spectral TCFs are expressed here as the sum of the constituent pair and triplet and quadruplet correlations. It has been shown that this sum cancels completely for the QID mechanism at long time[6] even though the individual parts do not vanish. It is of interest to study the time-derivative components TCFs in the region of this cancellation to see if there is an analogous behavior in this alternative representation. In addition, several assumptions concerning correlations of linear or angular velocities of different molecules may be verified. For example, it is often assumed that velocities of different particles are not correlated. Although this is certainly true for TCFs in the limit of zero time where all variables are in an equilibrium ensemble, velocity cross correlations need not vanish for finite time intervals, as has been demonstrated in various publications concerning relative velocity TCFs for dense inert gases.[7] Thus, a careful study of such correlations is of interest, especially in the present case where the time dependence of the TCFs is sensitive to both velocities and functions of the coordinates.

The TCFs for the QID moments and their component n-body ($n = 2-4$) contributions have been simulated previously for liquid CS_2.[6,8] It has been shown that the collective TCF (the experimentally observable one) exhibits major destructive interferences between the n-body correlations. The separation of the molecular polarizability tensors into their scalar and second-rank parts shows various differences in the interference scheme at short time, whereas the long time limit of the separate TCFs is characterized by the same perfect cancellation between the n-body terms that appear in the amplitude ratios of these terms for a perfect lattice.[6] Similar conclusions can be drawn from simulation studies of dipole-induced dipole (DID) light scattering in liquid CS_2.[9]

One of the reasons for studying the induced dipole TCFs for liquid CS_2 is that the optical anisotropy of this molecule is quite large, with the gas-phase value for the anisotropic polarizability γ exceeding the isotropic polarizability α_o ($\alpha_o = 8.95$ Å^3, $\gamma = 10.05$ Å^3 [10]). Furthermore, CS_2 is a linear molecule with considerable elongation (bond length $d_{CS} = 1.553$ Å [11]) and thus with large shape anisotropy. Consequently, one may anticipate that the role of the orientational degrees of freedom may be quite large in this system. Experimentally, several groups have published far-infrared absorption spectra for liquid CS_2,[12−14] and various simulation studies have been devoted to the QID absorption in this liquid.[6,8,15] Indeed, the simulated TCFs are quite complex, showing rather important orientational contributions that are difficult to sort out cleanly from the translational part of the decay. Evidently, a hypothesis that we wish to test is that the time-derivative TCFs might simplify this task.

The remainder of the present article is organized as follows. In section II, we describe the relation between the TCF for the system QID moment and its second time derivative. Formulas for the dipole moment velocities are deduced, and the objects of the present study, their TCFs, are introduced. Computational details are briefly summarized in section III followed by the presentation and discussion of the results in section IV.

II. Theoretical Background

A. QID Induction and Time Derivatives. The dipoles that give rise to the far-infrared absorption spectra of nonpolar liquids are mainly due to the electric fields of the charge distributions of the molecules in the fluid interacting with molecular polarizabilities $\boldsymbol{\alpha}_i$. When the effects of field gradients and higher polarizabilities are neglected, this induction can be described by expanding the charge distributions in terms of electrostatic multipole moments.[16] In the case of CS_2, the first nonvanishing multipole is the quadrupole tensor **Q** that produces a system dipole moment **M** in the liquid phase via the QID scheme. In terms of pair interactions, the QID can be written as

$$\boldsymbol{\mu}_{ij} = -\frac{1}{3}\boldsymbol{\alpha}_i(\hat{\mathbf{u}}_i)\cdot\mathbf{T}^{(3)}(\mathbf{r}_{ij}):\mathbf{Q}_j(\hat{\mathbf{u}}_j) \tag{8}$$

Here, the index j refers to the inducing particle with quadrupole moment $\mathbf{Q}_j$ and i refers to the receiving particle with polarizability $\boldsymbol{\alpha}_i$. The center of mass position vectors of these particles are $\mathbf{r}_j$ and $\mathbf{r}_i$, and their orientations are expressed by unit vectors $\hat{\mathbf{u}}_i$ and $\hat{\mathbf{u}}_j$ along the molecular axes, respectively. The tensor $\mathbf{T}^{(3)}$ depends on the intermolecular separation vector $\mathbf{r}_{ij} = \mathbf{r}_i - \mathbf{r}_j$ with Cartesian components (denoted by Greek superscripts)

$$T_{ij}^{\alpha\beta\gamma}(\mathbf{r}_{ij}) = \frac{\partial}{\partial r_{ij}^{\alpha}}\frac{\partial}{\partial r_{ij}^{\beta}}\frac{\partial}{\partial r_{ij}^{\gamma}}\frac{1}{r_{ij}} \tag{9}$$

For axially symmetric charge distributions, $\boldsymbol{\alpha}$ is defined by

$$\alpha_i^{\alpha\beta} = (\alpha_o - \gamma/3)\,\delta_{\alpha\beta} + \gamma\, u_i^{\alpha}\, u_i^{\beta} \tag{10}$$

Similarly, the elements of the quadrupole moment tensor are

$$Q_j^{\alpha\beta} = \frac{Q_o}{2}(3u_j^{\alpha}\, u_j^{\beta} - \delta_{\alpha\beta}) \tag{11}$$

for the gas-phase quadrupole moment Q_o ($Q_o = 9.3 \times 10^{-40}$ Cm^2 [17]). Equations 8−11 have been given in several publications. For a more detailed discussion, we refer to ref 15. The goal of the present article is to present and characterize the TCFs for the time derivatives of the induced dipoles of eq 8. The time dependence of $\boldsymbol{\mu}_{ij}$ is a consequence of the translational and rotational motions of $\mathbf{r}_{ij}$, $\hat{\mathbf{u}}_i$, and $\hat{\mathbf{u}}_j$. The translational velocity term contains the relative velocity $\mathbf{v}_{ij}$ of the pair ij defined as the difference in the individual linear velocities $\mathbf{v}_i$ and $\mathbf{v}_j$. The time-derivative operator acting on $\hat{\mathbf{u}}$ in space-fixed coordinates contains the cross product between the angular velocity $\boldsymbol{\omega}$ and $\hat{\mathbf{u}}$ [18]

$$\frac{\mathrm{d}\hat{\mathbf{u}}_i}{\mathrm{d}t} = \boldsymbol{\omega}_i \times \hat{\mathbf{u}}_i = \mathbf{l}_i \tag{12}$$

for which we will use the symbol $\mathbf{l}_i$ and terminology "orientational velocity" in the following. With these definitions, the dipole velocities $\dot{\mathbf{u}}_{ij}$ are obtained from eq 8 and split naturally into a translational term ${}^{(t)}\dot{\boldsymbol{\mu}}_{ij}$, with αth Cartesian component

$${}^{(t)}\dot{\mu}_{ij}^{\alpha} = -\frac{1}{3}\sum_{\beta\gamma\delta\epsilon}\alpha_i^{\alpha\beta}\, T_{ij}^{\beta\gamma\delta\epsilon}(\mathbf{r}_{ij})v_{ij}^{\epsilon}\, Q_j^{\gamma\delta} \tag{13}$$

and a pair of terms due to the orientational motion of particles i and j, ${}^{(ri)}\dot{\boldsymbol{\mu}}_{ij}$ and ${}^{(rj)}\dot{\boldsymbol{\mu}}_{ij}$, respectively:

$$^{(ri)}\dot{\boldsymbol{\mu}}_{ij}^{\alpha} = -\frac{1}{3}\sum_{\beta\gamma\delta}\gamma(u_i^{\alpha}\, l_i^{\beta} + u_i^{\beta}\, l_i^{\alpha})\, T_{ij}^{\beta\gamma\delta}(\mathbf{r}_{ij})Q_j^{\gamma\delta} \qquad (14)$$

$$^{(rj)}\dot{\mu}_{ij}^{\alpha} = -\frac{1}{3}\sum_{\beta\gamma\delta}\alpha_i^{\alpha\beta}\, T_{ij}^{\beta\gamma\delta}(\mathbf{r}_{ij})\frac{3Q_o}{2}(u_j^{\gamma}\, l_j^{\delta} + u_j^{\delta}\, l_j^{\gamma}) \qquad (15)$$

The fourth rank tensor $\mathbf{T}_{ij}^{(4)}$ in eq 13 is defined by

$$T_{ij}^{\alpha\beta\gamma\delta}(\mathbf{r}_{ij}) = \frac{\partial}{\partial r_{ij}^{\delta}}T_{ij}^{\alpha\beta\gamma}(\mathbf{r}_{ij}) \qquad (16)$$

It is important to note that the orientational time dependence of $^{(ri)}\dot{\mu}_{ij}$ is due to the rotation of the anisotropic part of the polarizability of i and that of $^{(rj)}\dot{\mu}_{ij}$ to the rotation of the quadrupole of j. These two contributions to the overall time dependence can be of very different magnitudes, as will be shown below. From the computational point of view, it is simpler to evaluate $C(t)$ directly from its definition (eq 1), since that only requires the sampling of μ_{ij} to obtain a single TCF from the molecular trajectories, whereas eq 4 requires a knowledge of $C(0)$ and also the numerical integration of a TCF, which is actually the sum of several translational and rotational terms. However, some advantages of eq 4 should be mentioned. For instance, TCFs for dynamic variables that depend on structural quantities can show very slow relaxation, especially in liquids at high densities and low temperature. As examples, one might cite the potential contribution to the Green−Kubo TCF for the shear viscosity[19,20] or the n-body TCFs in II DID light scattering[9,21] or QID far-infrared absorption.[6] The evaluation of these functions from eq 1 requires large computational efforts in order to achieve statistically satisfactory accuracies. Usually, such TCFs are characterized by a fast initial decay that changes to a slow relaxation at long time. Consequently, the time derivatives are expected to have large amplitudes at short times and only small contributions (if any) at long time. The integral in eq 4 will be determined in large part by the short time behavior of the $C^{(2)}(t)$, and it is possible that one can avoid the necessity of sampling TCFs with small amplitudes at long times.

B. Time Correlation Functions. In this section we break down $C^{(2)}(t)$ into a sum of TCFs for translation, rotation, and coupled translation−rotation velocities. Thus, we write the TCF for the collective dipole $C(t)$ explicitly in terms of the pair dipole

$$C(t) = \sum_{i,j',k,l'=1}^{N}\langle\boldsymbol{\mu}_{ij}(0)\cdot\boldsymbol{\mu}_{kl}(t)\rangle \qquad (17)$$

where the prime on the indices j and l indicate $j \neq i$ and $l \neq k$, respectively. The number of equal molecular indices defines two two-body, three three-body, and one four-body TCF. In each case, one has $\boldsymbol{\mu}_{ij}(0)$ correlated with another induced dipole. Remembering that $\boldsymbol{\mu}_{ij}(0)$ is the dipole induced through the polarizability of i by the quadrupole of j, one has two-body TCFs due first to correlation of this induced dipole with itself at some later time t (denoted by C_{2A}) and second, to correlation with $\boldsymbol{\mu}_{ji}(t)$, the dipole due to the quadrupole on i inducing a dipole in j (C_{2B}). The second of these TCFs vanishes unless there is correlation between the orientations of the quadrupoles on i and j; a correlation between polarizability orientations is not necessary because of the orientation-independent part of this tensor. The three three-body TCFs consist of correlation between $\boldsymbol{\mu}_{ij}(0)$ and first, $\boldsymbol{\mu}_{ik}(t)$, the dipole induced in i by the quadrupole of k (C_{3A}), second, $\boldsymbol{\mu}_{kj}(t)$, the dipole induced in k by the quadrupole of j (C_{3C}), and third, $\boldsymbol{\mu}_{ki}(t)$, the dipole induced in k by the quadrupole of i (C_{3B}). Of these, the first and third vanish unless the molecular quadrupoles are orientationally correlated. Finally, the four-body term is due to the correlation between $\boldsymbol{\mu}_{ij}(0)$ and a dipole on k that is induced by a fourth molecule l and clearly is nonzero only when the quadrupoles on j and l are orientationally correlated. We have reviewed this separation procedure here because it also applies to the TCFs for all the dipole velocities introduced in eqs 13−15.

One can now write the collective TCF for the dipole velocities as collective translational and rotational TCFs plus a collective coupling TCF. Thus,

$$C^{(2)}(t) = C^{\mathrm{trans}}(t) + C^{\mathrm{coup}}(t) + C^{\mathrm{rot}}(t) \qquad (18)$$

where the translational TCF is

$$C^{\mathrm{trans}}(t) = \sum_{i,j',k,l'=1}^{N}\langle^{(t)}\dot{\boldsymbol{\mu}}_{ij}(0)\cdot^{(t)}\dot{\boldsymbol{\mu}}_{kl}(t)\rangle \qquad (19)$$

Owing to the differences in the orientational velocities of particles i and j, the translation−rotation coupling TCF is the sum of cross correlations between the translational dipole velocities and contributions stemming from the orientational velocities, either of particle k (denoted by C^{trk}) or particle l (denoted by C^{trl}):

$$C^{\mathrm{coup}}(t) = \underbrace{2\sum_{i,j',k,l'=1}^{N}\left\langle^{(t)}\dot{\boldsymbol{\mu}}_{ij}(0)\cdot^{(rk)}\dot{\boldsymbol{\mu}}_{kl}(t)\right\rangle}_{C^{trk}(t)} + \underbrace{2\sum_{i,j',k,l'=1}^{N}\left\langle^{(t)}\dot{\boldsymbol{\mu}}_{ij}(0)\cdot^{(rl)}\dot{\boldsymbol{\mu}}_{kl}(t)\right\rangle}_{C^{trl}(t)} \qquad (20)$$

Finally, the rotational TCF is decomposed into the the autocorrelations for $^{(ri)}\dot{\boldsymbol{\mu}}_{ij}$ (denoted by C^{ri}) and $^{(rj)}\dot{\boldsymbol{\mu}}_{ij}$ (denoted by C^{rj}) as well as the cross correlation C^{rirj} between these two dipole velocities:

$$C^{\mathrm{rot}}(t) = \overbrace{\sum_{i,j',i,k'=1}^{N}\left\langle^{(ri)}\dot{\boldsymbol{\mu}}_{ij}(0)\cdot^{(ri)}\dot{\boldsymbol{\mu}}_{ik}(t)\right\rangle}^{C^{ri}(t)} + \overbrace{2\sum_{i,j',k,l'=1}^{N}\left\langle^{(ri)}\dot{\boldsymbol{\mu}}_{ij}(0)\cdot^{(rj)}\dot{\boldsymbol{\mu}}_{kl}(t)\right\rangle}^{C^{rirj}(t)} + \underbrace{\sum_{i,j',k,j'=1}^{N}\left\langle^{(ri)}\dot{\boldsymbol{\mu}}_{ij}(0)\cdot^{(rj)}\dot{\boldsymbol{\mu}}_{kj}(t)\right\rangle}_{C^{rj}(t)} \qquad (21)$$

All these time-dependent second moments contribute to $C^{(2)}(t)$ in the integral of eq 4. By the breaking of each collective TCF into its component n-body correlations, the contributions of distinct degrees of freedom to the collective QID TCF can be obtained, allowing one to generalize the information gained in studies of the usual spectral second moment (which equals $C^{(2)}(0)$ in the present notation).[22,23] Also, the evaluations of trans, rot, and coup terms in eqs 19−21 give insight into the relative importance of these degrees of freedom in the relaxation of $C(t)$.

III. Computational Details

The MD simulations have been performed with 256 molecules in a cubic box with the usual periodic boundary conditions and minimum image conventions. A cutoff sphere of half of the length of the simulation box was applied to all distant-dependent properties. Liquid CS_2 was modeled by the three-center (12/6) Lennard-Jones potential of ref 24, which already has been applied to several previous simulations of the spectroscopic

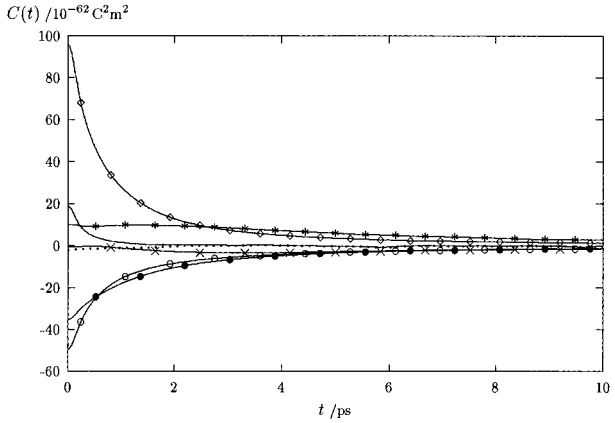

Figure 1. TCFs for the QID moment in liquid CS_2 simulated by correlating the dipoles from eq 8. The curves show the collective TCF (full line) and its breakdown into C_{2A} (full line with ◇), C_{2B} (full line with ○), C_{3A} (full line with ×), C_{3B} (full line with *), C_{3C} (full line with ●), and C_4 (dotted line). These TCFs are discussed in more detail in refs 6 and 8.

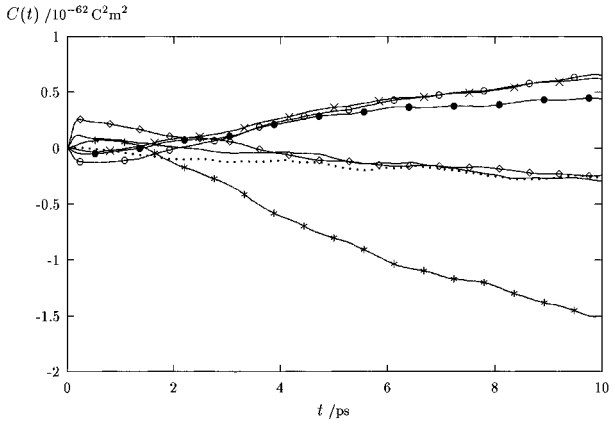

Figure 2. Differences in the two representations for the QID moment TCFs of Figure 1 obtained by subtracting the TCFs obtained from eq 4 from the TCFs in Figure 1. Line types and symbols for the functions are the same as in Figure 1.

properties of this liquid. The simulated thermodynamic state point corresponds to 298 K and liquid−vapor equilibrium (molar volume of 60.4 cm^3/mol). Calculated equilibrium properties of the liquid are in agreement with published results.[24] Equations of motion have been solved by a fifth-order predictor−corrector algorithm in time intervals of 3.5 fs. The TCFs specified in section II have been extended to 10 ps with a resolution of 35 fs. Starting from independently generated liquid configurations, several trajectories of 50 000 time steps have been analyzed in order to achieve statistical accuracy in the collective TCFs.

IV. Results and Discussion

A. TCFs for the Dipole Velocities. In order to test the applicability of eq 4 to the TCFs obtained from the simulation, we show the collective TCF for the QID dipole moment given by eq 17 and its component n-body terms in Figure 1. The corresponding functions have also been evaluated by integrating eq 4 with simulated $C^{(2)}(t)$ calculated from eq 18. Performing the numerical integration by the trapezoidal rule, we find that the two long-time computations give curves that are indistinguishable on the scale of Figure 1. Nevertheless, the agreement between the two representations is not perfect. In Figure 2 we illustrate the differences between the two representations and find small systematic deviations between the two sets of TCFs

TABLE 1: Properties of the $C^{(2)}(t)$ from Eq 5[a]

TCF	$C^{(2)}(0)$	integral (eq 22)	integral (eq 23) − $C(0)$
$C^{(2)}$	840	−0.0	−0.5
$C^{(2)}_{2A}$	2037	0.2	3.9
$C^{(2)}_{2B}$	−856	−0.2	−3.7
$C^{(2)}_{3A}$	22.5	−0.1	−2.9
$C^{(2)}_{3B}$	−1.4	0.3	−3.1
$C^{(2)}_{3C}$	−333	−0.2	−4.6
$C^{(2)}_4$	−28.1	0.0	0.2

[a] Given are the initial amplitudes $C^{(2)}(0)/10^{-62}$ C^2 m^2 ps^{-2} and the integrals defined by eqs 22 and 23 in units of 10^{-62} C^2 m^2 ps^{-1} and 10^{-62} C^2 m^2, respectively.

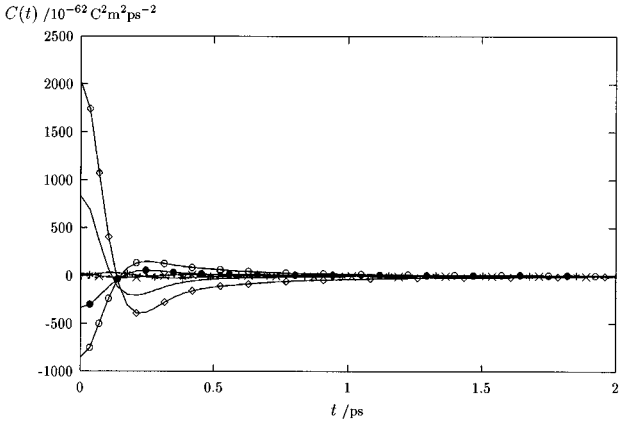

Figure 3. Collective TCF for the dipole moment velocities from eq 5 (full line) and its breakdown into the $C^{(2)}_{2A}$ (full line with ◇), $C^{(2)}_{2B}$ (full line with ○), $C^{(2)}_{3A}$ (full line with ×), $C^{(2)}_{3B}$ (full line with *), $C^{(2)}_{3C}$ (full line with ●) and $C^{(2)}_4$ (dotted line).

that appear at times longer than the decay time of the $C^{(2)}(t)$ and increase more or less linearly with time. These discrepancies are probably due to errors in the numerical integration procedure for the kernel $(t - \tau)C^{(2)}(\tau)$ and are extremely small on the scale of Figure 1. There are two exact conditions on $C^{(2)}(t)$ that are relevant:

$$\int_0^\infty C^{(2)}(\tau)\, d\tau = 0 \tag{22}$$

for $C(\infty) = 0$, and

$$C(0) + \int_0^\infty \tau C^{(2)}(\tau)\, d\tau = 0 \tag{23}$$

Equation 22 is well-known. Vanishing integrals of the force and torque auto-TCFs that give the second derivatives for velocity and angular velocity TCFs, respectively, are examples. Equation 23 follows directly from eqs 4 and 22. Table 1 shows the results of numerical tests of these relations for $C^{(2)}(\tau)$, together with the zero-time values of these functions. Equation 22 is very well obeyed, with deviations being very close to the estimated uncertainties in the simulations. Equation 23 is slightly less well obeyed because the weight factor of τ places more emphasis on the long-time tails of the $C^{(2)}(\tau)$ where the uncertainty is greater. Note that the deviations shown in Figure 2 are of the form expected for times long compared to the decay time of $C^{(2)}(\tau)$, where eq 4 gives a constant term plus a term that increases linearly with t with a slope equal to the the integrated area of $C^{(2)}(\tau)$. In fact, the slopes predicted from Table 1 do not agree very well with those obtained from Figure 2, which means only that the two long-time calculations are really beyond the limit of accurate evaluation.

Figure 3 shows the time evolution of the second time derivative of the QID TCFs. The breakdown into the component

n-body terms brings out three major contributions to the collective function: $C_{2A}^{(2)}$, $C_{2B}^{(2)}$, and $C_{3C}^{(2)}$, which also have been demonstrated to determine the short-time behavior of the QID moment.[6,8] These three TCFs quickly change sign and give well-defined extrema between 0.2 and 0.25 ps. The other two three-body TCFs and the four-body term are almost negligible. However, $C_{3A}^{(2)}$ and $C_{3B}^{(2)}$ are slightly structured in the first 0.5 ps whereas the four-body term presents only fluctuations about a vanishing average amplitude. Note that the averages over velocities in a TCF should vanish at zero time except when there are one or more pairs of velocity for the same particle. For example, $\langle v_{ij}^2 \rangle$ or $\langle \omega_i^2 \rangle$. Thus, the translational parts of the three-body terms do not vanish at zero time. Of the three three-body terms, only $C_{3C}^{(2)}$ involves the square of $\langle \omega_i^2 \rangle$ for a single molecular quadrupole; $C_{3A}^{(2)}$ involves the square of this quantity for a rotating anisotropic polarizability; $C_{3B}^{(2)}$ involves the square of this quantity for a quadrupole and an anisotropic polarizability, both on the same molecule. Compared to that of the rotating quadrupoles, the anisotropy of the polarizability will give a small contribution. The zero-time values for these functions listed in Table 1 conform reasonably well with this. Although the four-body function has a predicted zero value, it is not exactly zero. One must remember that it has not been calculated directly; in fact, it is the remainder after one subtracts the directly simulated two-body and three-body functions from the directly simulated total TCF. In general, the nonzero results obtained here for predicted zero quantities can be taken to be a measure of the precision of the simulations.

In Figure 3 it is apparent that the total second time derivative TCFs decay rapidly to small amplitudes in contrast to the QID TCFs that exhibit significant long-time correlations in the *n*-body terms in Figure 1. The second time derivatives are almost completely decorrelated at $t < 2$ ps. The long-time tails in the QID *n*-body TCFs for this liquid have been described elsewhere by exponential decays with relaxation rates of approximately 8 ps.[6] Consequently, the second derivatives are expected to present an exponential decay with roughly $^1/_{64}$ of the QID long-time amplitudes. We have not been able to detect this in the *n*-body contributions to the $C^{(2)}$ because of statistical uncertainties. For example, consider C_{2A}, which exhibits an initial amplitude of 100×10^{-62} C^2 m^2 and a long-time amplitude on the order of 5×10^{-62} C^2 m^2 (Figure 1). The long-time tail of $C_{2A}^{(2)}$ in Figure 2 should appear with an amplitude of $^5/_{64} \times 10^{-62}$ C^2 m^2 ps^{-2}, a value that disappears in the statistical fluctuations of this term. (A study at higher densities, where the long-time tails in the QID many-body terms appear with larger amplitudes[6] might verify an exponential decay in the corresponding $C^{(2)}$.)

The amplitude of the collective $C(0)$ and $C^{(2)}(0)$ can be experimentally determined from the experimental zeroth and second moments of the far-IR spectra. $C(0)$ determined in this way ranges from 9.6 [14] to 18.5×10^{-62} C^2 m^2.[13] The simulated value (18.7×10^{-62} C^2 m^2) is at the upper limit of the experimental range. The value of $C^{(2)}(0)$ that corresponds to the lower limit of the experimental $C(0)$ is 1080×10^{-62} C^2 m^2 ps^{-2},[14] almost 30% larger than our simulated result of 840×10^{-62} C^2 m^2 ps^{-2} (Table 2). It is likely that incorporating higher multipoles and polarizabilities in the induction mechanism would improve this situation.

Figure 3 indicates that the collective $C^{(2)}$ is primarily the result of cancellation between the positive $C_{2A}^{(2)}$ and the negative $C_{2B}^{(2)}$ and $C_{3C}^{(2)}$. Neglect of the other two three-body and the four-body terms does not significantly change the total $C^{(2)}$. However, the large cancellation makes it difficult to see what molecular relaxations are actually causing the decay of $C^{(2)}(t)$. As will be discussed below, all the TCFs from Figure 3 and Table 1 contain combinations of translational, rotational, and coupled translational−rotational contributions. In Figure 4, the separation of $C^{(2)}(t)$ into its collective translational, rotational, and translational−rotational parts is illustrated. The characteristics of these functions are summarized in Table 2. All these TCFs show extrema at roughly 0.2 ps. If we take the positions of the minima to be a measure of the time scale of the decay of these TCFs, we see that the decays in C^{trans} and C^{rot} are very similar, but the minimum of the C^{coup} is shifted by 0.1 ps toward smaller times. It is perhaps not surprising to see that the shapes of these translational and rotational functions are reminiscent of those of velocity autocorrelations in dense liquids. It indicates that the changes in the configurational parts of the TCFs are small on the time scale of the changes in the velocities. The effect of cancellations of the *n*-body components upon the decays of the collective TCFs remains to be discussed.

TABLE 2: Properties of the $C^{(2)}(t)$ from Eqs 18−21[a]

TCF	$C^{(2)}(0)$	integral (eq 22)
C^{trans}	335	13.4
C^{coup}	−1.8	−28.3
C^{trk}	−1.1	−4.0
C^{trl}	−0.7	−24.7
C^{rot}	507	14.6
C^{ri}	222	11.5
C^{rirj}	−258	−18.8
C^{rj}	543	21.8
$C^{(2)}$	840	0.0

[a] Given are the initial amplitudes $C^{(2)}(0)/10^{-62}$ C^2 m^2 ps^{-2} and the integral defined by eq 22 in units of 10^{-62} C^2 m^2 ps^{-1}.

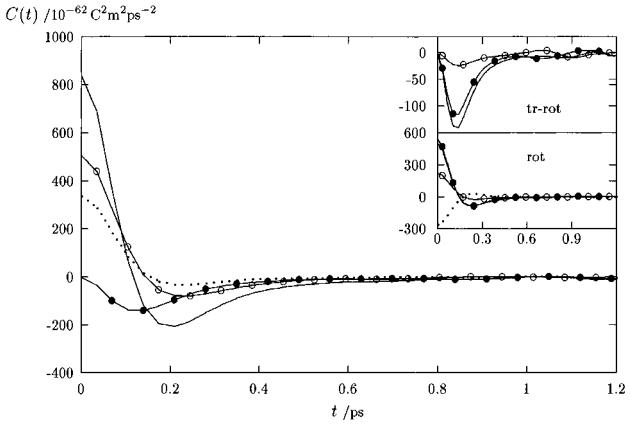

Figure 4. Collective TCFs for the dipole moment velocities from eq 18. Shown are $C^{(2)}$ (full line), C^{trans} (dotted line), C^{rot} (full line with ○), and C^{coup} (full line with ●). The upper inset gives the separation of the C^{coup} (full line) into C^{trk} (full line with ○) and C^{trl} (full line with ●) from eq 20. The lower inset shows the C^{ri} (full line with ○), C^{rj} (full line with ●), and C^{rirj} (dotted line) that make up C^{rot} (full line, indistinguishable from C^{rj}).

All the TCFs for the coupling of translational with rotational degrees of freedom are essentially zero at zero time, as required. The breakdown of C^{rot} and C^{coup} into contributions originating from the anisotropic polarizability (C^{ri},C^{trk}) or quadrupole moment (C^{rj},C^{trl}) demonstrates that the orientational variables associated with the quadrupole dominate C^{rot} and C^{coup}.

In a recent paper, Ladanyi and Klein have published TCFs for the polarizability anisotropy velocities corresponding to the second time derivative of light scattering TCFs for acetonitrile.[3] Although the situation in light scattering is different owing to the appearance of allowed orientational scattering, the overall features of the second derivative TCFs are similar to those presented in Figure 4.

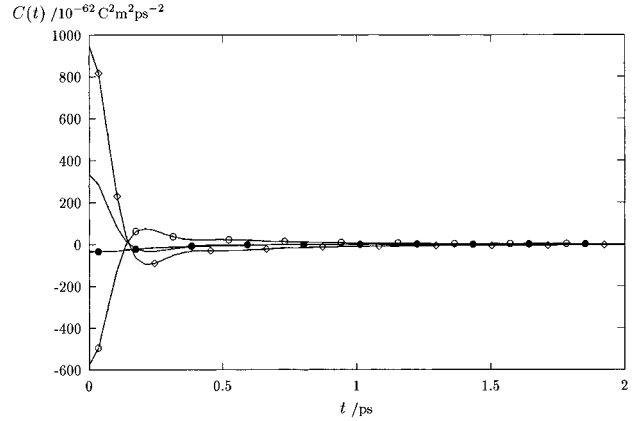

Figure 5. Collective TCF C^{trans} from eq 19 for the translational contribution to the dipole moment velocities (full line) and its breakdown into C_{2A}^{trans} (full line with ◇), C_{2B}^{trans} (full line with ○), and C_{3C}^{trans} (full line with ●). Note that C_{3A}^{trans}, C_{3B}^{trans}, and C_4^{trans} are very small and not shown.

TABLE 3: Initial Amplitudes of the *n*-Body Terms of the TCFs from Eqs 19−21 in Units of 10^{-62} C^2 m^2 ps^{-2}

TCF	C_{2A}	C_{2B}	C_{3A}	C_{3B}	C_{3C}	C_4
C^{trans}	951	−578	12.5	−9.7	−32.8	−7.9
C^{ri}	221	0.5	1.4	−1.2	2.6	−2.9
C^{rj}	864	2.4	9.0	−5.6	−303	−24.7
C^{rirj}	−1.7	−280	2.0	12.3	2.1	7.5
C^{trk}	0.9	−0.6	−1.4	1.1	−1.0	−0.1
C^{trl}	1.5	−1.0	−1.1	1.7	−1.9	0.1

In Table 2, the integrals of the TCFs in Figure 4 are listed. With exception of the total $C^{(2)}$, all these integrals are small but finite. Whereas the C^{trans} and C^{rot} integrals are positive, the C^{coup} integral is negative and cancels exactly the translational and rotational contributions, thus ensuring that the integral of $C^{(2)}$ vanishes. Finite integrals for these TCFs are expected because a vanishing integral is predicted only for the total time derivative of $C^{(2)}$.

B. Many-Body Translational Correlations. In Table 3, the initial amplitudes of the *n*-body TCFs contributing to the collective C^{trans} are listed. Evidently, correlations of type C_{3A}^{trans} and C_{3B}^{trans} as well as four-body correlations are of little importance. It was found that this is true not only for zero time but at all times considered. In Figure 5, the breakdown of the C_{trans} into its two long-time remaining two-body TCFs and C_{3C}^{trans} is illustrated. Whereas C_{3C}^{trans} relaxes from its initial amplitude almost completely within 1 ps, the two-body terms change sign at 0.2 ps and exhibit decays slower than the decay of C_{3C}^{trans}.

The two-body TCFs involve correlations of relative velocities for the same pair of molecules $\boldsymbol{v}_{ij}\cdot\boldsymbol{v}_{ij}$ and thus might be expected to show amplitudes larger than for the three-body terms with pairs of relative velocities such as $\boldsymbol{v}_{ij}\cdot\boldsymbol{v}_{ik}$. C_{2B}^{trans} appears with a sign opposite that of C_{2A}^{trans} owing to the exchange of the molecular indices i and j in the relative velocity. Beyond 0.5 ps, the two two-body terms cancel each other almost perfectly, producing a fast decay in the collective TCF.

C. Many-Body Rotational Correlations. In Figures 6−8, the breakdown of C^{ri}, C^{rj}, and C^{rirj} into their most important *n*-body terms is shown. The magnitudes of these functions at $t = 0$ are given in Table 3. The terms in these rotational TCFs that involve autocorrelations of the rotational velocities will be largest, especially at $t = 0$, and those with cross correlations of these velocities must vanish at $t = 0$. Thus, at $t = 0$ only the 2A and 3A TCFs for C^{ri} are finite and only the 2A and 3C TCFs for C^{rj} are finite. The results shown in Table 3 confirm this and, there and in Figure 6, indicate that $C_{3A}^{ri}(t)$ is nearly zero at all times but C_{3C}^{rj} is quite large. Since the velocities in the TCFs are the same, one must look to the configurational factors to understand the difference between the two TCFS. In fact, the difference is that the 3A TCF involves the orientational correlation of pairs of quadrupole moments on different molecules, and this is apparently quite small, whereas the 3C

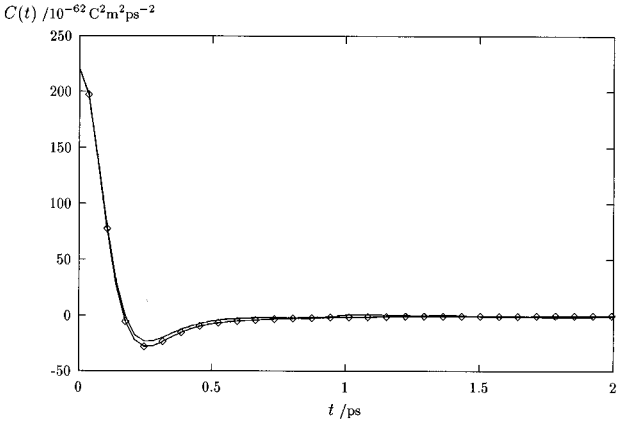

Figure 6. Collective TCF C^{ri} from eq 21 for the rotational contribution of particle i to the dipole moment velocities (full line) and its C_{2A}^{ri} term (full line with ◇).

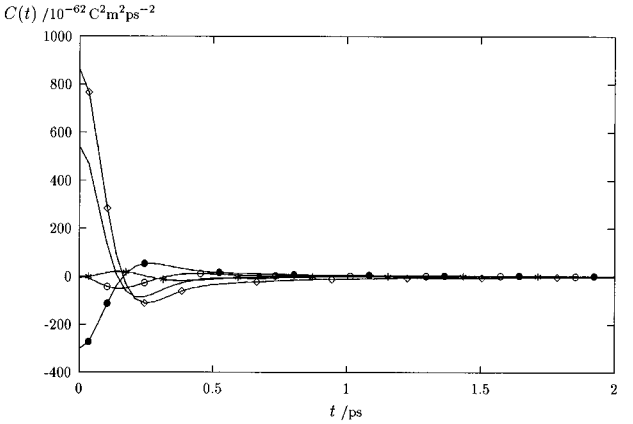

Figure 7. Collective TCF C^{rj} from eq 21 for the rotational contribution of particle j to the dipole moment velocities (full line) and its breakdown into C_{2A}^{rj} (full line with ◇), C_{2B}^{rj} (full line with ○), C_{3B}^{rj} (full line with *), and C_{3C}^{rj} (full line with ●). C_{3A}^{rj} and C_4^{rj} are very small and not shown.

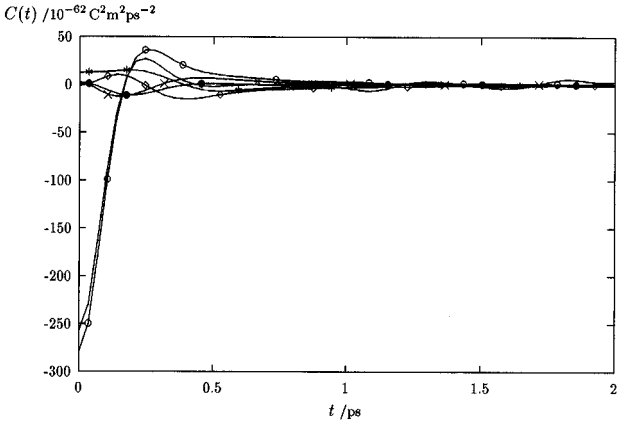

Figure 8. Collective TCF C^{rirj} (full line) from eq 21 that couples the rotational contributions of particles i and j to the dipole moment velocities. Its components C_{2A}^{rirj} (full line with ◇), C_{2B}^{rirj} (full line with ○), C_{3A}^{rirj} (full line with ×), C_{3B}^{rirj} (full line with *), and C_{3C}^{rirj} (full line with ●) are also shown. C_4^{rirj} is very small and is not plotted here.

TCFs involve correlations of the polarizability tensors of different molecules that contain isotropic parts that are unaffected by orientational correlations or the lack thereof. In the case of C^{rirj}, only the 2B and 3B are finite at $t = 0$, as is approximately confirmed in Table 3. Figure 8 shows again that the TCFs that are zero at $t = 0$ become small but finite at $t > 0$ among to the development and decay of cross correlation in their angular velocity factors.

The sums of these various TCFs give the collective C^{ri}, C^{rj}, and C^{rirj}. For C^{ri}, only one component TCF is important and there is no cancellation between *n*-body contributions. Figures 7 and 8 show that several *n*-body terms must be taken into account to obtain the collective C^{rj} and C^{rirj}. The collective C^{rj} is a consequence of destructive interferences between the sum of C^{rj}_{2A} and C^{rj}_{3B} on one side and the sum of C^{rj}_{2B} and C^{rj}_{3C} on the other.

In both C^{rj} and C^{rirj}, cancellation causes the collective function to become immeasurably small for $t > 0.5$ ps. Figures 6−8 show that the C^{rj} are much larger than C^{ri} and C^{rirj}. The C^{rj} depend upon the time dependence of the orientational velocity of the quadrupole moment, whereas the orientational velocities in C^{ri} are those for anisotropic polarizabilities. Evidently, the reorientations of the quadrupoles play a more important role in the QID spectra for CS_2 than the orientations of the anisotropic part of the molecular polarizability, and this is particularly true when the functions involved are in the form of autocorrelations.

D. Many-Body Correlations Due to Translation−Rotation Coupling. The two TCFs C^{trk} and C^{trl} that show the coupling between translational and rotational motions are presented in Figure 9. The definition of the translational and rotational dipole velocities in eqs 13−15 shows that correlations between linear velocities and angular velocities are involved in these TCFs. Consequently, the amplitudes of all the *n*-body C^{trk} and C^{trl} should be zero at $t = 0$. This is confirmed in Table 3 to the statistical accuracy of the simulation. However, all the component two- and three-body cross rotation−translation TCFs develop amplitudes in the first 0.5 ps. In the case of the C^{trl}_{2A} (the coupling of translational dipole velocities with quadrupole rotational velocity of particle *j*), the largest amplitude is observed with an absolute value of approximately 150×10^{-62} C^2 m^2 ps^{-2}. From Figure 9 it is evident that destructive interferences between the C^{trk}_{2A} and C^{trk}_{3B} on one side and the C^{trk}_{2B}, C^{trk}_{3A}, and C^{trk}_{3C} on the other are involved in the collective C^{trk}. The same situation holds for C^{trl}. Thus, with exception of the four-body terms, all the *n*-body contributions must be considered. In contrast to most of the *n*-body contributions to the translational and rotational TCFs shown in Figures 5−8, the *n*-body coupling terms do not change sign and thus exhibit no cancellation. Thus, one expects important translational−rotational coupling contributions to the total QID TCF in liquid CS_2. However, these are dynamical correlations that must be zero at zero time and in the limit of infinite time. The extrema in the C^{trl} are of larger amplitudes than in the corresponding C^{trk} because the full polarizability tensor is involved in the rotational dipole velocities entering the C^{trl} whereas the dipole velocities depending on the orientational velocities of particle *k* only contain anisotropic polarizability contributions. The existence of cross correlations between linear and angular velocities at finite times has been discussed in the literature.[26,27] For linear molecules, this cross TCF has been evaluated in a moving molecular reference frame.[28] Although the TCFs of the present study are obtained in the laboratory system, the shape of the C_{2A} in both panels of Figure 9 resembles the cross TCF for linear and angular velocities found in ref 28. However, it is important to realize

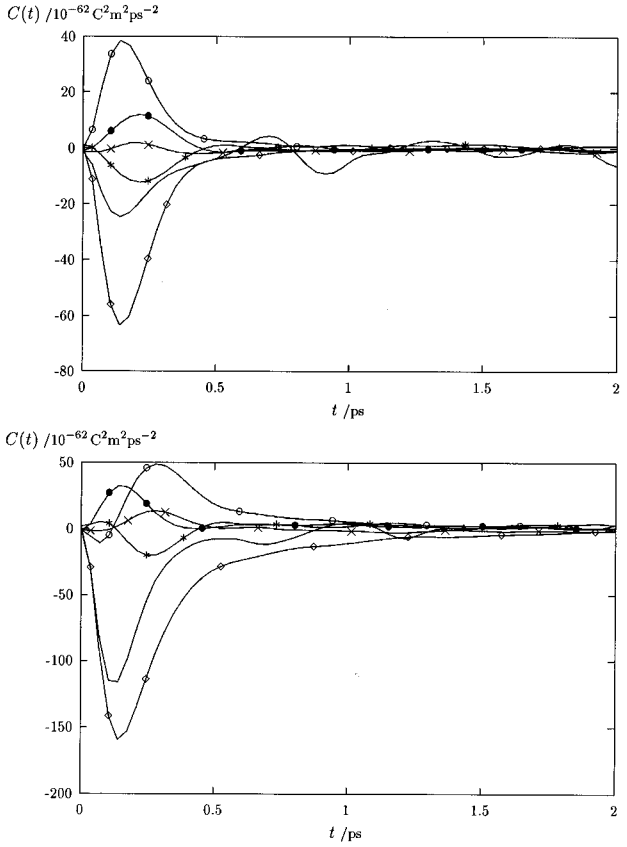

Figure 9. Collective TCF that couples the translational and rotational parts of the dipole moment velocities (full line) and its breakdown into C_{2A} (full line with ◇), C_{2B} (full line with ○), C_{3A} (full line with ×), C_{3B} (full line with *), and C_{3C} (full line with ●). The four-body contributions are not given. The coupling of translational dipole velocities with rotational velocities of particle *k*, the C^{trk}, is illustrated in the upper panel, and the coupling of translational dipole velocities to the rotational velocities of particle *l*, the C^{trl}, is given in the lower panel.

that velocity TCFs need not exhibit the same time dependence as those for the various *n*-body terms that make up the time dependence of the II dipole TCF.

V. Conclusions

The second time derivatives of the QID moment TCFs for the thermodynamic state point at 298 K have been obtained from MD computer simulations for liquid CS_2. Numerical integration of these TCFs reproduces the characteristics of the QID TCFs. Small deviations between the integrated second time derivatives and the QID TCFs at long times are likely due to artifacts introduced by the numerical integration especially in the component *n*-body terms that exhibit long-time QID correlations. The second time derivatives decorrelate on a faster time scale than the QID TCFs, favoring an accurate calculation of QID TCFs using the TCFs for the dipole velocities. Long-time tails in the *n*-body TCFs for the dipole velocities have not been observed at the thermodynamic state studied here but might appear at higher densities. Thus, exponential long-time decays observed in the *n*-body TCFs for the QID moments[6] cannot be confirmed in the present study. The universal cancellation observed (to date) in the *n*-body tails means of course that the tails of the collective functions are extremely small and have no significant effect on the spectral profiles obtained from the Fourier transforms of the TCFs.

The breakdown of the TCFs for the dipole velocities into contributions stemming from translational and orientational

velocities shows that the large spectral moments for CS_2 at 298 K (which correspond to the second derivative amplitudes at $t = 0$ shown in Figure 4) are due to translational and orientational contributions in roughly equal parts. Indeed, perhaps the most significant result of this calculation is given in Figure 4, where the collective trans, rot, and coup parts of the II dipole spectral $C^{(2)}$ TCF are to be found. The relative importance of these three terms varies with time, but it can be seen that, for liquid CS_2, the trans and the rot contributions to the total TCF are comparable in magnitude and in their changes with time. Since the coup term must be zero at $t = 0$, its time dependence is quite different from the other two functions. It interesting to note that coup is negative at all times, and that all three TCFs are nearly equal at $t \approx 0.2$ ps so that their sum produces a relatively deep minimum in the second derivative spectral TCF at that time. Thus, one concludes that the importance of the coup terms depends very much upon the time. Reasons for the behavior of the collective functions are to be found in the curves for their component parts that are shown in Figures 5−8, but the (rigorous) breakdown of the spectral TCF into its trans, rot, and coup $C^{(2)}$ contributions is unique to the reformulation used in this paper. Furthermore, this reformulation is sufficiently general to allow its use in the analysis of numerous other dynamical properties of fluids. These include II light scattering TCFs and the transport coefficients shear viscosity and thermal conductivity. (We are presently simulating these other properties using this reformulation.) Observables showing simpler, noncollective character are limited: tracer diffusion and orientational TCFs for allowed infrared and light scattering spectra. The TCFs appearing in the theory of solvation dynamics[3,29,30] are being rewritten in terms of the second derivative TCFs and fall into the category of non-collective functions.

In the case of the translational contributions, autocorrelations of linear velocities are involved in the two- and three-body terms. However, the weakness of the correlation of molecular orientation of different molecules, which is present in the C_{3A}^{trans} and C_{3B}^{trans}, reduces the amplitudes of these two TCFs. Consequently, one can adequately express the collective translational TCF as the sum of C_{2A}^{trans}, C_{2B}^{trans}, and C_{3C}^{trans}.

In the case of the rotational contributions, different terms with different features must be considered. For example, orientational autocorrelations of the quadrupole moments are present in C_{2A} and exhibit large amplitudes in both the *ri* and *rj* TCFs.

The component cross correlations between translational and orientational dipole velocities exhibit, as expected, negligible amplitudes at $t = 0$, but all these component two- and three-body TCFs develop correlations in the first 0.5 ps. Although the cross C_{2A} has a shape similar to the cross TCF between linear and angular velocities,[28] this is not the case for the other *n*-body terms evaluated here. The observed collective translation−rotation coupling is complex not only because the coupling is dynamic but also because the property for which the coupling is calculated is made up of a sum of *n*-body terms.

The integrals of the collective and *n*-body TCFs for the total dipole velocities vanish. However, integrals of the translational and rotational contributions as well as the cross terms between the two are large and are positive in the case of translational and rotational contributions and exactly cancelled by the negative integral over the cross TCFs that couple translational and rotational correlations. One can best characterize the rates of rotational and translational motion in this liquid by the decay rates of the individual *n*-body C^{trans}, C^{ri}, and C^{rj} shown in Figure 5−7. Judging by the extrema in the individual functions, it appears that the decays of these TCFs are all very similar—there is no separation of translational and rotational time scales in liquid CS_2. It should be emphasized that these conclusions depend upon the particular observable under investigation as well as the temperature and density of the liquid. However, the method of analysis developed here is sufficiently general and sufficiently rigorous to allow one to undertake comparative studies of different properties and different liquids over ranges of temperature and density in the expectation of useful physical insights into the nature of molecular motion in these systems.

Acknowledgment. Financial support of the present study from the CNPq (Process 301165/94-7) and the chemistry section of the NSF (Grant CHE 900-4073) and the generous allocation of CPU time and computational facilities by the national supercomputer center (CESUP) in Porto Alegre are gratefully acknowledged.

References and Notes

(1) Balucani, U.; Zoppi, M. *The Dynamics of the Liquid State*; Clarendon: Oxford, 1994; Appendix J.
(2) Keyes, T. *J. Chem. Phys.* **1996**, *104*, 9349.
(3) Ladanyi, B. M.; Klein, S. *J. Chem. Phys.* **1996**, *105*, 1552.
(4) Steele, W. A. *Mol. Phys.* **1987**, *61*, 1031.
(5) Mc Quarrie, D. A. *Statistical Mechanics*; Harper & Row: New York, 1976; Chapter 20.
(6) Stassen, H.; Steele, W. A. *Mol. Phys.*, **1996**, *89*, 1603.
(7) Balucani, U.; Vallauri, R.; Murthy, C. S. *J. Chem. Phys.* **1982**, *77*, 3233. Posch, H. A.; Balucani, U.; Vallauri, R. *Physica A* **1984**, *123*, 516.
(8) Samios, J.; Mittag, U.; Dorfmüller, Th. *Mol. Phys.* **1986**, *59*, 65. Fujita, Y.; Ikawa, S. *J. Chem. Phys.* **1995**, *103*, 9580.
(9) Stassen, H.; Steele, W. A. *J. Chem. Phys.* **1995**, *103*, 4408.
(10) Bogaard, M. P.; Buckingham, A. D.; Pierens, R. K.; White, A. H. *J. Chem. Soc., Faraday Trans.* 1 **1978**, *74*, 3008.
(11) Zandler, M. E.; Watson, J. A., Jr.; Eyring, H. *J. Phys. Chem.* **1968**, *72*, 2730.
(12) Davies, G. J.; Evans, M. *J. Chem. Soc., Faraday Trans.* 2 **1976**, *72*, 1194. Potthast, L.; Samios, J.; Dorfmüller, Th. *Chem. Phys.* **1986**, *102*, 147. Marteau, Ph.; Obriot, J.; Occelli, R.; Bose, T. K.; Gherfi, A.; St Arnaud, J. M. *J. Mol. Liq.* **1989**, *43*, 193.
(13) Zoidis, E.; Samios, J.; Dorfmüller, Th. *Chem. Phys.* **1992**, *168*, 349.
(14) Fujita, Y.; Ikawa, S. *J. Chem. Phys.* **1995**, *103*, 3907.
(15) Madden, P. A.; Tildesley, D. J. *Mol. Phys.* **1983**, *49*, 193. Dorfmüller, Th.; Samios, J. *Mol. Phys.* **1984**, **53**, 1167.
(16) Gray, C. G.; Gubbins, K. E. *Theory of Molecular Fluids, Vol. 1: Fundamentals*; Clarendon: Oxford, 1984; Chapter 2.
(17) Amos, R. D.; Battaglia, M. R. *Mol. Phys.* **36**, 1517 (1978).
(18) Goldstein, H. *Classical Mechanics*; 2nd ed.; Addison-Wesley: Reading, MA 1980; Chapter 4.
(19) Hoheisel, C. *Theoretical Treatment of Liquids and Mixtures*; Elsevier: New York, 1993.
(20) Stassen, H.; Steele, W. A. *J. Chem. Phys.* **1995**, *102*, 932; **1995**, *102*, 8533.
(21) Ladd, A. J. C.; Litovitz, T. A.; Montrose, C. J. *J. Chem. Phys.* **1979**, *71*, 4242. Mueller, A.; Steele, W. A.; Versmold, H. *J. Chem. Phys.* **1993**, *99*, 4993. Keller, M.; Mueller, A.; Versmold, H.; Steele, W. A. *J. Chem. Phys.* **1995**, *103*, 8854.
(22) Keller, M.; Mueller, A.; Versmold, H.; Steele, W. A. *J. Chem. Phys.* **1995**, *103*, 8854.
(23) Mueller, A.; Reh, M.; Röder, M.; Steele, W.; Versmold, H. *Mol. Phys.* **1995**, *85*, 233.
(24) Tildesley, D. J.; Madden, P. A. *Mol. Phys.* **1981**, *42*, 1142.
(25) Tildesley, D. J.; Madden, P. A. *Mol. Phys.* **1983**, *48*, 129.
(26) Evans, G. T. *Mol. Phys.* **1978**, *36*, 65. Evans, M. W.; Ferrario, M.; Grigolini, P. *Mol. Phys.* **1980**, *39*, 1369.
(27) Steele, W. A.; Vallauri, R. *Mol. Phys.* **1987**, *61*, 1019.
(28) Ryckaert, J. P.; Bellemanns, A.; Cicotti, G. *Mol. Phys.* **1981**, *44*, 979.
(29) Ladanyi, B. M.; In *Electron and Ion Transfer in Condensed Matter*; Kornshev, A. A.; Ulstrup, J., Eds.; World Scientific: Singapore, 1997.
(30) Ladanyi, B. M.; Maroncelli, M. P., In preparation.